Flow properties of driven-diffusive lattice gases: Theory and computer simulation

Debashish Chowdhury[1] and Jian-Sheng Wang[2]
[1]*Department of Physics, Indian Institute of Technology, Kanpur 208016, India*
[2]*Department of Computational Science, National University of Singapore, Singapore 119260, Republic of Singapore*
(Received 14 August 2001; published 4 April 2002)

We develop n-cluster mean-field theories ($1 \leqslant n \leqslant 4$) for calculating the *flux* and the *gap distribution* in the nonequilibrium steady states of the Katz-Lebowitz-Spohn model of the driven diffusive lattice gas, with attractive and repulsive interparticle interactions, in both one and two dimensions for arbitrary particle densities, temperature as well as the driving field. We compare our theoretical results with the corresponding numerical data we have obtained from the computer simulations to demonstrate the level of accuracy of our theoretical predictions. We also compare our results with those for some other prototype models, notably particle-hopping models of vehicular traffic, to demonstrate the qualitative features we have observed in the Katz-Lebowitz-Spohn model, emphasizing, in particular, the consequences of *repulsive* interparticle interactions.

DOI: 10.1103/PhysRevE.65.046126 PACS number(s): 05.50.+q, 05.60.−k, 45.70.Vn

I. INTRODUCTION

The driven-diffusive lattice gas models are of current interest in nonequilibrium statistical mechanics [1–4]. Depending on the nature of the drive, these driven-dissipative systems can attain steady states that are far from equilibrium. The simplest driven-diffusive lattice gas model that incorporates interparticle interactions is the Katz-Lebowitz-Spohn model [5] (from now onwards referred to as KLS). Some of the particle-hopping models of vehicular traffic [6] are closely related to some special limits of the KLS model in one dimension. Therefore, in order to compare and contrast the spatiotemporal organizations and the flow properties of the KLS model with those in the particle-hopping models of vehicular traffic, we calculate here those properties of the KLS model that are important from the perspective of vehicular traffic.

Over the last decade extensive investigations of vehicular traffic have been made using the so-called particle-hopping models that represent each vehicle by a particle [6–8]. All these traffic models are defined on discrete lattices each site of which, in the spirit of the lattice gas models, represents a cell that can accommodate at most one particle at a time. In almost all the standard particle-hopping models of vehicular traffic the only nonvanishing interparticle interaction is the mutual hard-core repulsion that is usually implemented through the condition of exclusion principle: no two particles are allowed to occupy the same lattice site simultaneously. Therefore, a comparison of our results on the KLS model with the corresponding results for the particle-hopping models of vehicular traffic will show the effects of interparticle interactions other than mere hard-core repulsion.

The flux (per lane) is defined to be the number of particles (per lane) crossing a detector site per unit time. In the context of vehicular traffic [9], the most important quantity of interest is the so-called *fundamental relation* that depicts the dependence of the flux on the density of the vehicles. The number of empty sites in between a pair of particles is usually taken as a measure of the corresponding distance headway (DH).

In this paper we theoretically calculate the DH distributions and the flux in the steady states of the KLS model, separately for attractive and repulsive interparticle interactions, within the framework of a *cluster mean-field theory* (MFT) [4,10–14] which has been very successful also in the theoretical treatment of the particle-hopping models of vehicular traffic [6,15–17]. We also indicate the level of the accuracy of our cluster-MFT results by comparing these with the corresponding numerical data obtained from our computer simulations of the KLS model.

The organization of this paper is as follows. In Sec. II we define the KLS model and some related particle-hopping models that are relevant for our discussion in the subsequent sections. We summarize in Sec. III the methods of the cluster MFT we use for our theoretical calculations as well as those of computer simulation. In Secs. IV, V, and VI, we present our theoretical results for the one-dimensional KLS model (both with attractive and repulsive interactions) in the 1-cluster, 2-cluster, and 4-cluster approximations, respectively, together with the corresponding numerical data from our computer simulations. We present our results for the two-dimensional KLS model in Sec. VII. We compare and contrast the results for the KLS model with the corresponding results for the particle-hopping models of vehicular traffic in Sec. VIII before summarizing the main results in the concluding Sec. IX.

II. THE MODELS

A. The KLS model

Suppose the variable c_i describes the state of occupation of the site i ($i=1,2,\ldots,N$) on a discrete lattice; c_i is allowed to take one of the only two values, namely, $c_i=1$ if the site i is occupied by a particle and $c_i=0$ if it is empty (or, equivalently, occupied by a ''hole''). The Hamiltonian for the system, in the absence of any external driving field, is given by

$$\mathcal{H} = -4J \sum_{\langle ij \rangle} c_i c_j , \tag{1}$$

where the summation on the right hand side is to be carried

out over all the nearest-neighbor pairs and J takes into account the corresponding interparticle interactions.

The KLS model can be recast in the language commonly used in the theory of magnetism by using classical Ising spin variables $S_i=(2c_i-1)$ where $S_i=1$ and $S_i=-1$ represent the particles and holes, respectively, and the corresponding Hamiltonian, in the absence of the external drive, is given by

$$\mathcal{H}' = -J\sum_{\langle ij\rangle} S_i S_j . \tag{2}$$

The *attractive* and *repulsive* interparticle interactions, captured by $J>0$ and $J<0$, respectively, in the Hamiltonian (1) correspond to the ferromagnetic and antiferromagnetic interactions in the form (2) of the Hamiltonian.

However, throughout the rest of this paper, we shall use the particle-hole picture, where the instantaneous state (configuration) of the system at time t is completely described by $(\{c\};t)$. For example, in case of a system of length L in dimension $d=1$, $(\{c\};t)\equiv(c_1,c_2,\ldots,c_L;t)$. Similarly, for the $L_x\times L_y$ square lattice $(\{c\};t)\equiv(c_{11},c_{12},\ldots,c_{ij},\ldots,c_{L_xL_y};t)$. The average density c of the particles is given by $c=\lim_{N\to\infty,L\to\infty} N/N_s=\lim_{N\to\infty,L\to\infty}(\Sigma_i^{N_s}c_i)/N_s$ where N_s, the total number of available sites, is L for a linear chain and L^2 for a square lattice of size $L\times L$. Note that, because of the conservation of the particles, the density c is conserved by the dynamics.

The dynamics of the system is governed by the well-known Kawasaki dynamics: at any nonzero temperature T, a randomly chosen nearest-neighbor particle-hole pair is exchanged with the probability $\min[1,e^{-\beta(\Delta\mathcal{H}+\not{E})}]$ where $\beta=(k_BT)^{-1}$ (k_B being the Boltzmann constant) and $\Delta\mathcal{H}=\mathcal{H}(\{c\}_{new})-\mathcal{H}(\{c\}_{old})$ is the difference in the energy of the new and old configurations while $\not{E}=(-1,0,+1)$ for jumps, respectively, along, transverse to, against the direction of the driving field $\vec{E}$. Throughout this paper we take $k_B=1$ and express the temperature T in the units of J.

For the KLS model with *attractive* interparticle interactions ($J>0$) on a square lattice, there is not only an ordered state at all $T<T_c(E)$, but the critical temperature $T_c(E)$ increases with E, saturating at a value $T_c(E\to\infty)\simeq 1.4T_c(E=0)$ where $T_c(E=0)$ is the critical temperature of the corresponding Ising model in thermodynamic equilibrium [1,5,18]. On the other hand, $T_c(E)$ decreases with E when the interparticle interactions are *repulsive* (i.e., $J<0$); the ordering is altogether destroyed by sufficiently large E. However, there is no ordered structure at any nonzero temperature in the one-dimensional KLS model, irrespective of the sign of the interaction J. Because of this intrinsic qualitative difference in the nature of the ordering in the steady states in $d=1$ and $d=2$ we present the corresponding results in separate sections.

B. The totally asymmetric simple exclusion process

In the totally asymmetric simple exclusion process (from now onwards referred to as TASEP) [19], initially, N classical particles occupy *randomly* the sites of a one-dimensional lattice of length $L(\geqslant N)$. One time step of the dynamics consists of updating the position of N particles picked up in a random-sequential manner; each randomly chosen particle moves forward, with probability q, if the lattice site immediately in front of it is empty. For this model, the simple single-site (i.e., 1-cluster) MFT [20] gives the *exact* flux

$$F=qc(1-c) \tag{3}$$

for all densities c of the particles.

C. Comparison between the models

In the special case $E=0$ the KLS model reduces to the corresponding standard Ising model in thermodynamic equilibrium. Note that in $d=1$, in the opposite limit $E\to\infty$ the hopping against the driving field becomes impossible and, moreover, the field E dominates so overwhelmingly over $\Delta\mathcal{H}$ at all nonzero temperatures T that, in this limit, the one-dimensional KLS model reduces to the TASEP, with $q=1$, irrespective of the sign of the interaction J, provided J remains *finite*. For all the nonvanishing finite E, in the limit $J=0$, the one-dimensional KLS model reduces to the ASEP with the hopping probability $q=\min\{1,e^{-\not{E}/k_BT}\}$. Finally, at infinitely high temperatures each particle moves completely randomly, independent of each other, with equal probability in all directions.

III. METHODS OF CALCULATION

In this section we briefly outline the methods of our analytical as well as numerical calculations.

A. Cluster-mean-field theory

The dynamical cluster MFT has been used successfully in the analytical treatments of several nonequilibrium models including, for example, surface-reaction models [10] and particle-hopping models of vehicular traffic [15–17]. However, in all the traffic models there is no interparticle interaction except, of course, the hard-core repulsion. Moreover, unlike the traffic models, the particles in the KLS model can also move against the drive.

In this paper we extend the approach in appropriate manner to calculate the flux F as a function of c in the KLS model for arbitrary $J\neq 0$, $0\leqslant T\leqslant\infty$, and $\vec{E}\neq 0$.

We define an n cluster ($n<N$) to be a collection of n sites each of which is the nearest neighbor of at least another site belonging to the same cluster. For simplicity of notation, let us consider $d=1$. We denote the probability of finding an n cluster in the state $(c_1,c_2,\ldots,c_n)$ at time t by the symbol $P_n(c_1,c_2,\ldots,c_n;t)$. We treat an n cluster exactly and approximate all the $(n+m)$ cluster probabilities by a product of n-cluster probabilities in a manner so as to couple the n-cluster to the rest of the system self-consistently (see, for example, [6] for a pedagogical introduction and the existing literature).

It is straightforward to see that the state of the 2 cluster (c_i,c_{i+1}) at time $t+\Delta t$ depends on the state of the 4 cluster $(\tau_{i-1},\tau_i,\tau_{i+1},\tau_{i+2})$ at time t so that the exact master equation

$$\left[\frac{dP_2(c_i,c_{i+1})}{dt}\right]=\sum_{\tau_{i-1},\tau_{i+2}}[P_4(\tau_{i-1},c_{i+1},c_i,\tau_{i+2})w(\tau_{i-1},c_{i+1},c_i,\tau_{i+2})-P_4(\tau_{i-1},c_i,c_{i+1},\tau_{i+2})w(\tau_{i-1},c_i,c_{i+1},\tau_{i+2})]$$
$$+\sum_{\tau_{i-1},\tau_{i-2}}[P_4(\tau_{i-2},c_i,\tau_{i-1},c_{i+1})w(\tau_{i-2},c_i,\tau_{i-1},c_{i+1})-P_4(\tau_{i-2},\tau_{i-1},c_i,c_{i+1})w(\tau_{i-2},\tau_{i-1},c_i,c_{i+1})]$$
$$+\sum_{\tau_{i+2},\tau_{i+3}}[P_4(c_i,\tau_{i+2},c_{i+1},\tau_{i+3})w(c_i,\tau_{i+2},c_{i+1},\tau_{i+3})-P_4(c_i,c_{i+1},\tau_{i+2},\tau_{i+3})w(c_i,c_{i+1},\tau_{i+2},\tau_{i+3})] \quad (4)$$

governing the time evolution of the 2-cluster probabilities $P_2(c_i,c_{i+1})$ involves the 4-cluster probabilities $P_4(\tau_{i-1},\tau_i,\tau_{i+1},\tau_{i+2})$ for all those configurations that can lead to the 2-cluster configuration $(c_i,c_{i+1};t)$ under consideration

$$w(\tau_1,\tau_2,\tau_3,\tau_4)=W(\tau_1,\tau_2,\tau_3,\tau_4\rightarrow\tau_1,\tau_3,\tau_2,\tau_4)$$
$$=\min(1,\exp\{\beta J[(\tau_1\tau_3+\tau_2\tau_4)$$
$$-(\tau_1\tau_2+\tau_3\tau_4)+(\tau_2-\tau_3)E]\}) \quad (5)$$

are the corresponding transition probabilities. However, the master equation governing the time evolution of the 4-cluster probabilities $P_4(\tau_{i-1},\tau_i,\tau_{i+1},\tau_{i+2})$ involve 6-cluster probabilities, and so on. A few concrete examples of such exact master equations for n-cluster probabilities are given in the Appendix A. In the spirit of the cluster-mean-field approach, we truncate this hierarchy of exact master equations by expressing, albeit approximately, all the $(n+m)$-cluster probabilities in terms of the n-cluster probabilities.

According to the definition of DH, the probability for a DH of j is given by

$$P(j)=P(\underline{1}|\underbrace{0000\cdots0}_{j\ \text{times}}\ \ 1). \quad (6)$$

We evaluate the right hand side of the Eq. (6) in the 2-cluster and 4-cluster approximations.

B. Computer simulation

In our computer simulations, we begin with initial conditions where the particles are arranged randomly on a lattice of linear size L (i.e., the system is a linear chain of size L in $d=1$ and square lattice of size $L\times L$ in $d=2$). The system is then allowed to evolve, following the Kawasaki exchange algorithm with the METROPOLIS probabilities $\min[1,e^{-\beta(\Delta\mathcal{H}+\not{E})}]$ mentioned above, for time steps of the order of 10^4, so as to allow it to reach its steady state and, then, for further 10^5 steps during which the time-averaged flux is measured. Finally, for the same set of values of the parameters, this process is repeated for 100 different initial configurations to compute the configuration-averaged flux. Since we did not observe any significant difference between the results for $L=10^4$ and $L=10^5$ in $d=1$ and between those for $L=50$ and $L=100$ in $d=2$ all the data presented in this paper were generated using $L=10^4$ in $d=1$ and $L=50$ in $d=2$.

IV. 1-CLUSTER APPROXIMATION IN ONE DIMENSION

It has been realized for some time [1] that the smallest cluster one must consider in a dynamical cluster MFT depends on the nature of the dynamics. Since the Kawasaki dynamics conserves the number of particles, in principle, the smallest cluster must consist of at least one *pair* of sites. However, it is also known that for the $E\rightarrow\infty$ limit of the KLS model, which is exactly identical with the TASEP (with $q=1$), the single-site MFT gives the exact result. Therefore, in this short section we not only establish explicitly the limitations of the 1-cluster MFT at weak E but also demonstrate how the accuracy of the 1-cluster MFT increases with increasing E in the KLS model in $d=1$.

The net flux is obtained from $F=F_f-F_r$ where the forward flux (i.e., flux in the direction of $\vec{E}$) is given by

$$F_f=\sum_{c_{i-1},c_{i+2}}P_4(c_{i-1},1,0,c_{i+2})w(c_{i-1},1,0,c_{i+2}), \quad (7)$$

while the reverse flux (i.e., the flux against $\vec{E}$) is given by

$$F_r=\sum_{c_{i-1},c_{i+2}}P_4(c_{i-1},0,1,c_{i+2})w(c_{i-1},0,1,c_{i+2}). \quad (8)$$

In the 1-cluster approximation the 4-cluster probabilities $P_4(c_{i-1},c_i,c_{i+1},c_{i+2})$ are approximated by the products of corresponding 1-cluster probabilities. Therefore, utilizing the facts that $P_1(1)=c$ and $P_1(0)=1-c$, in the 1-cluster approximation, the Eqs. (7) and (8) give, respectively,

$$F_f=\sum_{c_{i-1},c_{i+2}}P_1(c_{i-1})c(1-c)P_1(c_{i+2})w(c_{i-1},1,0,c_{i+2}) \quad (9)$$

and

$$F_r=\sum_{c_{i-1},c_{i+2}}P_1(c_{i-1})(1-c)cP_1(c_{i+2})w(c_{i-1},0,1,c_{i+2}) \quad (10)$$

for the forward and reverse flux. Hence, the net flux is

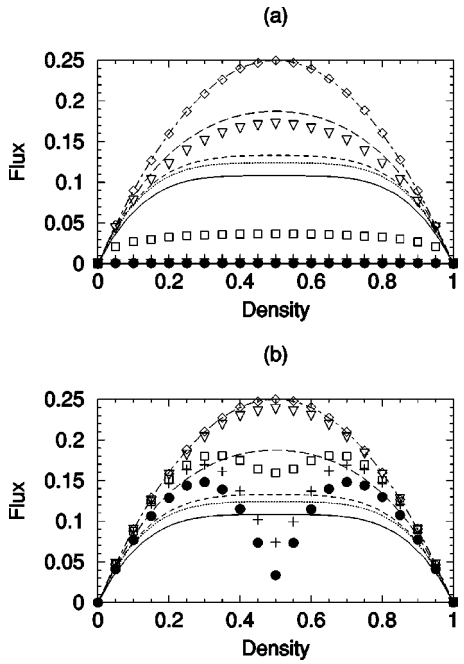

FIG. 1. Variation of the *net* flux F with the density c of the particles in the *steady state* of the one-dimensional KLS model with (a) attractive (i.e., ferromagnetic) interaction $J=1.0$ and (b) repulsive (i.e., antiferromagnetic) interaction $J=-1.0$, both at $T=0.5|J|$. In both (a) and (b) the discrete data points have been obtained from our computer simulations with $E=1.0(\bullet)$, $2.0(+)$, $3.0(\square)$, $4.0(\triangledown)$, and $100.0(\diamond)$, respectively. The lines represent the predictions of the 1-cluster approximation for $E=1.0$ (solid line), 2.0 (dotted line), 3.0 (dashed line), 4.0 (long dashed), and 100.0 (dot dashed), respectively.

$$F=c(1-c)\{(2c^2-2c+1)(\min[1,e^{\beta E}]-\min[1,e^{-\beta E}]) + c(1-c)(\min[1,e^{\beta(E-4J)}]-\min[1,e^{\beta(-E+4J)}] - \min[1,e^{\beta(-E-4J)}]+\min[1,e^{\beta(E+4J)}])\}. \quad (11)$$

The expression (11) predicts that the net flux F is independent of the sign of the interaction J, at all c and T, irrespective of the strength of E; this is certainly not true in general, except at very large E (Fig. 1). A comparison between the theoretical prediction (11) and the results of our computer simulations (Fig. 1) exposes not only the quantitative inaccuracy of the 1-cluster MFT but also its failure to account for the qualitative features of $F(c)$ in the case of repulsive interparticle interactions.

The fact that the 1-cluster MFT works better for stronger E is not surprising as the one-dimensional KLS model reduces to the TASEP (with $q=1$) in the limit $E\to\infty$ and it is well known that 1-cluster MFT gives exact result for the TASEP. Thus, Fig. 1 establishes the existence of strong correlations that are neglected by the 1-cluster MFT.

V. 2-CLUSTER APPROXIMATION IN ONE-DIMENSION

In the 2-cluster approximation, we approximate the 4-cluster probabilities, appearing in the exact master equation for the 2-cluster probabilities, by a product of 2-cluster probabilities, i.e.,

$$P_4(\tau_{i-1},\tau_i,\tau_{i+1},\tau_{i+2}) \propto P_2(\tau_{i-1},\tau_i)P_2(\tau_i,\tau_{i+1})P_2(\tau_{i+1},\tau_{i+2}), \quad (12)$$

or, more precisely,

$$P_4(\tau_{i-1},\tau_i,\tau_{i+1},\tau_{i+2}) = P_2(\tau_{i-1}|\underline{\tau_i})P_2(\tau_i,\tau_{i+1})P_2(\underline{\tau_{i+1}}|\tau_{i+2}). \quad (13)$$

Next, we parametrize the 2-cluster probabilities as follows:

$$P_2(0,0)=1-c-a, \quad (14)$$

$$P_2(1,1)=c-a, \quad (15)$$

where

$$P_2(1,0)=P_2(0,1)=a. \quad (16)$$

This parametrization enables us to satisfy the three constraints [15], namely, $\Sigma_{c_{i+1}=0}^{1}P_2(1,c_{i+1})=P_1(1)=c$, $\Sigma_{c_{i+1}=0}^{1}P_2(0,c_{i+1})=P_1(0)=1-c$, and $P_2(1,0)=P_2(0,1)$. Equivalently, these constraints also imply that

$$dP_2(0,0)/dt=dP_2(1,1)/dt=-dP_2(0,1)/dt =-dP_2(1,0)/dt.$$

So, only one of the four equations represented by Eq. (4) can be taken as an independent equation. Thus, the calculation of the four 2-cluster probabilities boils down to the calculation of the single parameter a.

Using MATHEMATICA for an automated generation of the equations and simplification, we find that, in the steady state, a satisfies the quadratic equation

$$Aa^2+Ba+C=0, \quad (17)$$

where

$$A=\min[1,e^{\beta(-E-4J)}]+\min[1,e^{\beta(E-4J)}]-\min[1,e^{\beta(-E+4J)}] - \min[1,e^{\beta(E+4J)}], \quad (18)$$

$$B=-(\min[1,e^{\beta(-E-4J)}]+\min[1,e^{\beta(E-4J)}]), \quad (19)$$

$$C=c(1-c)\{\min[1,e^{\beta(-E-4J)}]+\min[1,e^{\beta(E-4J)}]\}, \quad (20)$$

and, hence, taking the physical solution that allows the 2-cluster probabilities to be between 0 and 1, we get

$$a=(-B-\sqrt{B^2-4AC})/(2A). \quad (21)$$

The corresponding form of $P_2(1,0)$ for an alternative choice of w was derived by Szabo *et al.* [12]. Both the forms (21) and the Eq. (13) in Ref. [12] are special cases of the general form [21]

$$a=[1-\sqrt{1-2c(1-c)\kappa}]/\kappa \tag{22}$$

where

$$\kappa=2\left[1-\frac{w(\Delta H,-E)+w(\Delta H,+E)}{w(-\Delta H,-E)+w(-\Delta H,+E)}\right], \tag{23}$$

$w(\Delta H,\pm E)$ being the hopping probabilities against and along the field E, respectively.

Finally, in the 2-cluster MFT, the forward flux and the reverse flux are given by

$$F_f=\sum_{c_{i-1},c_{i+2}} P_2(c_{i-1}|\underline{1})P_2(1,0)P_2(\underline{0}|c_{i+2}) \times w(c_{i-1},1,0,c_{i+2}) \tag{24}$$

and

$$F_r=\sum_{c_{i-1},c_{i+2}} P_2(c_{i-1}|\underline{0})P_2(0,1) \times P_2(\underline{1}|c_{i+2})w(c_{i-1},0,1,c_{i+2}), \tag{25}$$

respectively; the net flux is obtained from $F=F_f-F_r$.

In the following few sections we compare the predictions of this 2-cluster MFT with the corresponding numerical data obtained from our extensive computer simulations of the KLS model.

A. Fundamental diagrams for arbitrary E at $T>0$

It is straightforward to verify that at an infinitely high temperature the expressions (24) and (25) for F_f and F_r become identical and, therefore, the net flux vanishes; high temperature not only washes away the effects of J, as it is known to do even in equilibrium, but also the effects of E making particle movement in both directions equally probable.

In Fig. 2 we plot the flux as a function of the particle density c, at a fixed nonzero finite temperature T, for five different values of E; the agreement between the theoretical prediction and computer simulation is very good for both attractive [Fig. 2(a)] as well as repulsive [Fig. 2(b)] interactions.

The $F(c)$ curves are the analogues of the fundamental relations for the traffic models. The shape of the curve $F(c)$ in the KLS model with *attractive* ($J>0$) is qualitatively similar to those observed in the particle-hopping models of vehicular traffic. In sharp contrast, we find a qualitatively different shape of the curve $F(c)$ in the KLS model with *repulsive* interactions ($J<0$); there is a minimum, rather than maximum, at $c=1/2$ provided the strength of J is comparable to that of E. Moreover, for the same T and E, the flux is higher in the case of *repulsive* interparticle interactions than that in the case of *attractive* interparticle interactions. Nevertheless, because of the particle-hole symmetry, the curves in both the Figs. 2(a) and 2(b) are symmetric about $c=1/2$ irrespective of the sign of the interparticle interactions.

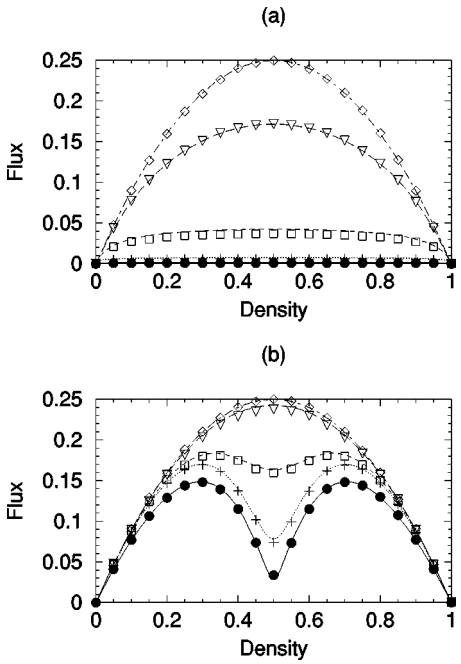

FIG. 2. Variation of the *net* flux F with the density c of the particles in the *steady state* of the one-dimensional KLS model with (a) attractive interaction $J=1.0$ and (b) repulsive interaction $J=-1.0$, both at $T=0.5|J|$. In both (a) and (b) the discrete data points, have been obtained from our computer simulations with $E=1.0(\bullet)$, $2.0(+)$, $3.0(\square)$, $4.0(\triangledown)$, and $100.0(\diamond)$, respectively. The lines represent the corresponding predictions of the 2-cluster approximation.

Also note that in both the Figs. 2(a) and 2(b) $F(c=1/2,E)\to 1/4$ as $E\to\infty$. This is a consequence of the fact that, as stated before, the KLS model reduces to the TASEP, with $q=1$, in the limit $E\to\infty$ (in both the cases of attractive and repulsive interparticle interactions) as long as J and T remain finite. In fact, in all the Figs. 1(a), 1(b) and 2(a), 2(b), the full curve $F(c,E\to\infty)$ is given by exact expression $F(c,E\to\infty)=c(1-c)$.

Thus, unlike the 1-cluster MFT, the 2-cluster MFT reproduces the qualitative features of the $F(c)$ curves for all E and for both attractive as well as repulsive interactions. Moreover, the flux predicted by the 2-cluster MFT is also in good quantitative agreement with the corresponding computer simulation data, except for a narrow range of c about $c=1/2$. This indicates that the predictions of 2-cluster MFT, although quite accurate for arbitrary E, is *not exact* (except, of course, $E\to\infty$) for the KLS model in $d=1$. We shall improve our theory further by developing a 4-cluster MFT in the following section.

In order to get a deeper insight into the dependence of the flux $F(c,E,T)$ on c,E,T as well as on the sign of J we analyze the results of the 2-cluster MFT in detail in a few special limits in the following sections.

B. Flux at $T=0$

Let us investigate the dependence of the flux $F(c,E,T=0)$ on the driving field E at $T=0$ for arbitrary values of c. For *repulsive* interparticle interactions, the 2-cluster expres-

sions (18)–(20) for A, B, and C reduce to the simple forms $A=2$, $B=-2$, $C=2c(1-c)$ for all $E<4|J|$, $A=1$, $B=-2$, $C=2c(1-c)$ at $E=4|J|$, and to the forms $A=0$, $B=-1$, $C=c(1-c)$ for all $E>4|J|$. Substituting the zero-temperature values of A, B, and C into the Eq. (21), we find that, at $T=0$, for all $E<4|J|$ $a\equiv P_2(1,0)=c$ for $c<1/2$, and $a\equiv P_2(1,0)=1-c$ for $c>1/2$; physically, this means that when less than half of the sites are occupied by particles (holes), both the nearest neighbors of each particle (hole) are *certainly* holes (particles) because of the repulsive nature of the interparticle interaction. On the other hand, at $T=0$, for all $E>4|J|$, $a\equiv P_2(1,0)=c(1-c)$ for any arbitrary c; this implies that at $T=0$ the effects of all $E>4|J|$ is equivalent to those of infinitely large E at all finite nonzero T so that 1-cluster MFT becomes exact. Moreover, at $T=0$, for $E=4|J|$, $a\equiv P_2(1,0)=1-\sqrt{1-2c(1-c)}$ for all c.

Substituting the appropriate expression of a, derived above for $T=0$, into the limiting form of the net flux $F(c,E,T=0)$, obtained from the 2-cluster expressions (24) and (25), we get

$$F(c,E,T=0)=\begin{cases} F^r_<(c) & \text{for } E<4|J| \\ F^r_=(c) & \text{for } E=4|J| \\ F^r_>(c) & \text{for } E>4|J|, \end{cases} \tag{26}$$

for the KLS model with *repulsive* interparticle interactions at $T=0$, where

$$F^r_<(c)=\theta(0.5-c)\left[\frac{c}{1-c}(1-2c)\right] + \theta(c-0.5)\left[\frac{1-c}{c}(2c-1)\right], \tag{27}$$

$$F^r_=(c)=\frac{2\{2c(1-c)-1\}+2\sqrt{1-2c(1-c)}\{1-c(1-c)\}}{c(1-c)}, \tag{28}$$

and

$$F^r_>(c)=c(1-c), \tag{29}$$

$\theta(x)$ being the step function, namely, $\theta(x)=0$ for all $x<0$ and $\theta(x)=1$ for all $x>0$.

In the special case of half-filling, the particles remain ''pinned'' to their respective positions by the interparticle interactions J and no $E<4|J|$ is strong enough to cause any ''depinning.'' Such ''switching'' of the flux from zero to a nonzero value *discontinuously*, in response to the driving field E, has been reported earlier for the KLS model on a linear chain [12] as well as on a square lattice [10].

In sharp contrast to the c dependence of $F^r_<(c)$ in the case of *repulsive* interparticle interactions, we have $F^a_<(c)=0$ for all c when the interparticle interaction is *attractive*; therefore, in the latter case,

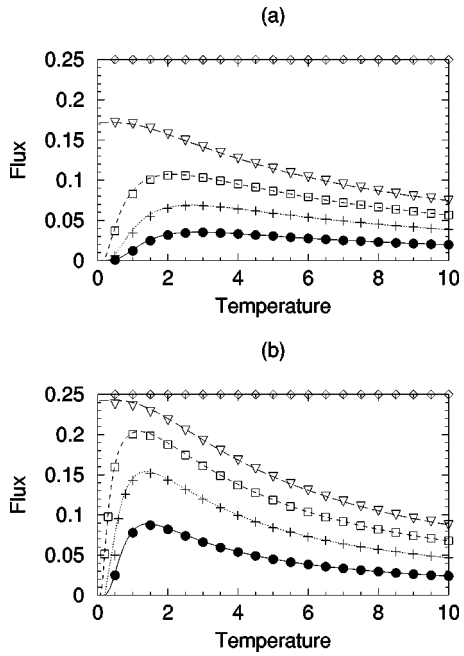

FIG. 3. Variation of the *net* flux F with the temperature T in the *steady state* of the one-dimensional KLS model with (a) attractive interaction $J=1.0$ and (b) repulsive interaction $J=-1.0$, both at $c=0.5$. In both (a) and (b) the discrete data points have been obtained from our computer simulations with $E=1.0$(●), 2.0(+), 3.0(□), 4.0(▽), and 100.0(◇), respectively. The lines represent the corresponding predictions of the 2-cluster approximation.

$$F(c,E,T=0)=\begin{cases} F^a_<(c) & \text{for } E<4|J| \\ F^a_=(c) & \text{for } E=4|J| \\ F^a_>(c) & \text{for } E>4|J|, \end{cases} \tag{30}$$

for the KLS model with *attractive* interparticle interactions at $T=0$, where

$$F^a_<(c)=0, \tag{31}$$

$$F^a_=(c)=\frac{\{2c(1-c)+1\}-\sqrt{1+4c(1-c)}}{2c(1-c)}, \tag{32}$$

and

$$F^a_>(c)=c(1-c). \tag{33}$$

At $T=0$, all $E>4|J|$ is equivalent to $E\to\infty$, irrespective of the sign of J and, hence, the corresponding flux is $c(1-c)$.

C. Temperature dependence of flux

In this section we consider the dependence of F on T at a few special values of c. As demonstrated in the Figs. 3–7, the predictions of the 2-cluster theory agree very well with the corresponding numerical data obtained from our computer simulations.

The nonmonotonic variation of the flux with temperature at small and intermediate values of E is an interesting phe-

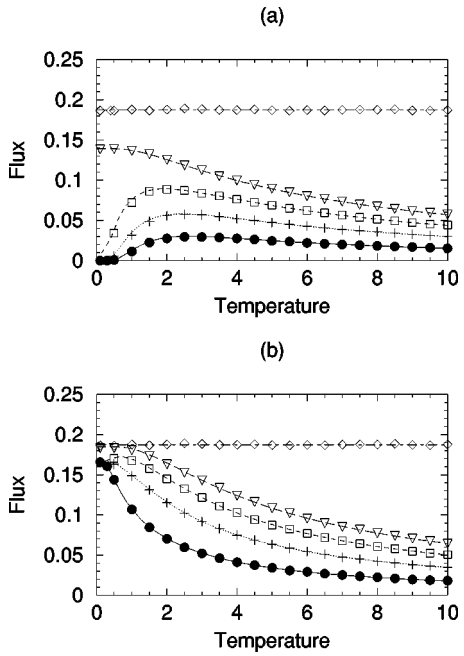

FIG. 4. Same as in Fig. 3, except that the density of the particles is $c=0.25$.

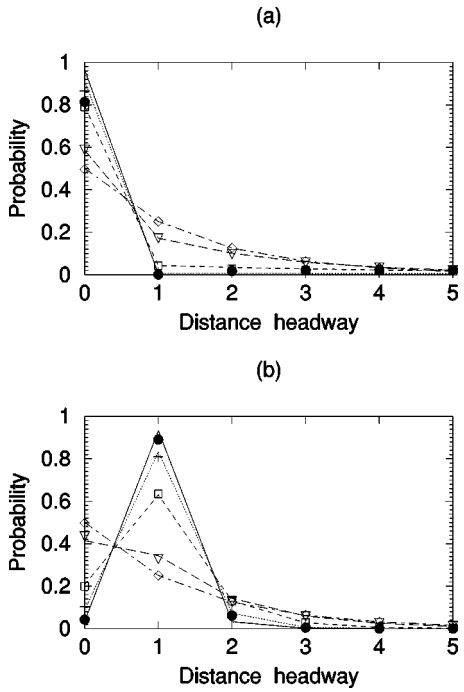

FIG. 5. The distance-headway distribution in the *steady state* of the one-dimensional KLS model with (a) attractive interaction $J=1.0$ and (b) repulsive interaction $J=-1.0$, both at $c=1/2$ and $T=0.5|J|$. In both (a) and (b) the discrete data points have been obtained from our computer simulations with $E=1.0(\bullet)$, $2.0(+)$, $3.0(\square)$, $4.0(\triangledown)$, and $100.0(\diamond)$, respectively. The lines represent the corresponding predictions of the 2-cluster approximation.

nomenon. So long as T is nonzero but much smaller than E, it works against J and helps in ''depinning'' the particles that can move forward under the influence of the driving field E. However, when T becomes much larger than E, then it washes out the effect of E allowing particles to move against $\vec{E}$ as often as along $\vec{E}$.

D. DH distribution

In the 1-cluster approximation, the DH distribution is given by

$$P_{1c}(j)=c(1-c)^j. \tag{34}$$

However, in the 2-cluster approximation, we write

$$P_{2c}(j)=P_2(\underline{1}|1) \quad \text{for } j=0 \tag{35}$$

and

$$P_{2c}(j)=P_2(\underline{1}|0)\{P_2(\underline{0}|0)\}^{j-1}P_2(\underline{0}|1) \quad \text{for } j\geqslant 1. \tag{36}$$

Hence, in the 2-cluster approximation, we get

$$P_{2c}(j)=1-\frac{a}{c} \text{ for } j=0 \tag{37}$$

whereas

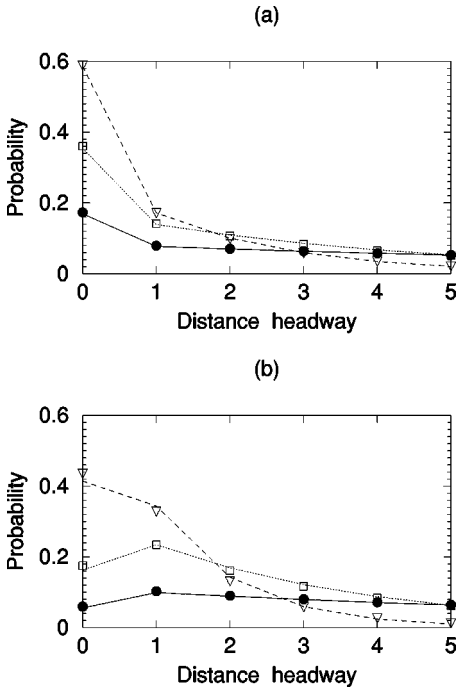

FIG. 6. The distance-headway distribution in the *steady state* of the one-dimensional KLS model with (a) attractive interaction $J=1.0$ and (b) repulsive interaction $J=-1.0$, both for $E=4.0$ and $T=0.5|J|$. In both (a) and (b) the discrete data points have been obtained from our computer simulations with $c=0.1(\bullet)$, $0.25(\square)$, and $0.5(\triangledown)$, respectively. The lines represent the corresponding predictions of the 2-cluster approximation.

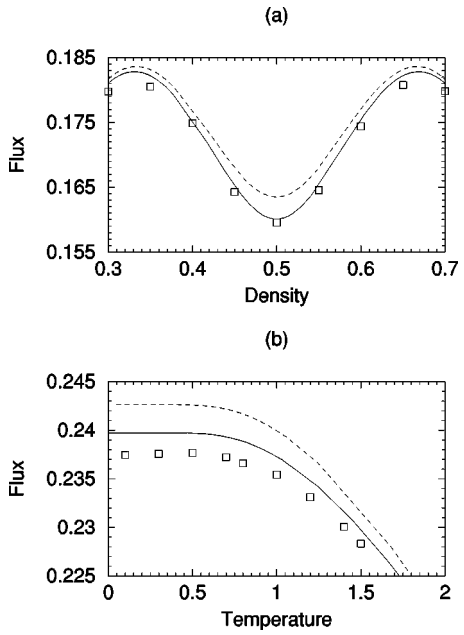

FIG. 7. Comparison of the predictions of 2-cluster and 4-cluster MFTs on the variation of the *net* flux F with (a) the density and (b) temperature in the *steady-state* of the one-dimensional KLS model with repulsive interaction $J=-1.0$. The parameters in (a) are $T=0.5, E=3.0$ while those in (b) are $c=0.5, E=4.0$. The dashed and solid lines are the theoretical results obtained in the 2-cluster and 4-cluster approximations, respectively, whereas the discrete data points are the numerical data obtained from our computer simulations.

$$P_{2c}(j)=\frac{a^2}{c(1-c)}\left[1-\frac{a}{1-c}\right]^{j-1} \quad \text{for } j\geqslant 1. \tag{38}$$

The variations of the DH distribution with E (for fixed c) and with c (for fixed E), as predicted by Eqs. (37) and (38) of the 2-cluster approximation, are compared with the corresponding computer simulation data in Figs. 5 and 6, respectively. Note that for $c=0.5$, in the absence of E, the most probable DH is $j=0$ or $j=1$ depending on whether the interaction is attractive (i.e., ferromagnetic, in the language of magnetism) or repulsive (i.e., antiferromagnetic). This type of spatial organization of the particles persists even in the presence of E as long as E is much weaker than the strength of the interaction J (see Fig. 5). However, deviation from this spatial organization increases gradually with increasing strength of E. In the limit $E\to\infty$, for all finite $|J|$, the DH distribution approaches the exact DH distribution of the TASEP and, as expected, is independent of the sign of the interaction J. For a given E, which is comparable with the strength $|J|$ of the interaction, increasing c leads to more congestion and, therefore, the probability of having a DH $=0$ becomes larger for higher c (see Fig. 6).

VI. 4-CLUSTER APPROXIMATION IN ONE DIMENSION

The exact master equation for the 4-cluster probabilities (given in the Appendix B), as expected on general grounds, involve 6-cluster probabilities. In the 4-cluster approximation we break up the 6-cluster probabilities in terms of the products of the 4-cluster probabilities using the prescription

$$\begin{aligned}P_6(\tau_{i-2},\tau_{i-1},\tau_i,\tau_{i+1},\tau_{i+2},\tau_{i+3})&=P_4(\tau_{i-2},\tau_{i-1}|\underline{\tau_i,\tau_{i+1}})P_4(\tau_{i-1},\tau_i,\tau_{i+1},\tau_{i+2})\\&\times P_4(\underline{\tau_i,\tau_{i+1}}|\tau_{i+2},\tau_{i+3}).\end{aligned} \tag{39}$$

Due to the constraints of conditional probabilities and conservation of total probabilities, at 4-cluster level, we have seven independent equations and the same number of variables. The solution is obtained by solving a set of nonlinear equations. We find that although the 4-cluster results are, clearly, an improvement over the 2-cluster results, the difference in the actual numerical values of the flux in the two approximations, for the same set of parameters, is extremely small. The flux obtained in these two approximations for a typical set of values of the parameters are compared in Fig. 7 (the corresponding differences in the DH distributions are too small to be shown in a figure).

It is worth pointing out that the 4-cluster approximation is not only a *quantitative* improvement over the 2-cluster approximation. The 4-cluster approximation can account for the forward-backward symmetry breaking, an interesting phenomenon [12,13], which the 2-cluster approximation fails to capture.

VII. CLUSTER APPROXIMATIONS IN TWO DIMENSION

It is well known [1] that, usually, the cluster MFT fails to account for the properties of the driven-diffusive lattice gases below the ordering temperature $T_c(E)$. Therefore, we confine our discussions in this section to temperatures $T>T_c(E)$.

As in $d=1$, for the same set of parameters, the flux in the two-dimensional KLS model with attractive interparticle interactions [Fig. 8(a)] is lower than that in the same model with repulsive interparticle interactions [Fig. 8(b)].

A comparison of the predictions of the cluster MFT with the computer simulation data [Fig. 8] establishes that, in the case of *attractive* interactions both the 1-cluster and 2-cluster MFT overestimate the flux, although the prediction of the 2-cluster theory is closer to the computer simulation data. On the other hand, in the case of *repulsive* interactions, the 1-cluster MFT gives an underestimate whereas the 2-cluster MFT provides an overestimate of the flux. The level of accuracy of the 2-cluster MFT can be estimated from the plots in Fig. 9; a close inspection, thus, reveals that the 2-cluster MFT does not reproduce the dip in the flux around $c=1/2$ in the case of repulsive interparticle interactions.

VIII. COMPARISON WITH THE RESULTS FOR OTHER MODELS

It is well established [20] that the 1-cluster MFT result [Eq. (3)] is the *exact* expression for the flux in TASEP. If the random-sequential updating of the TASEP is replaced by the parallel updating it becomes identical with the Nagel-Schreckenberg (NS) model [22] of vehicular traffic with

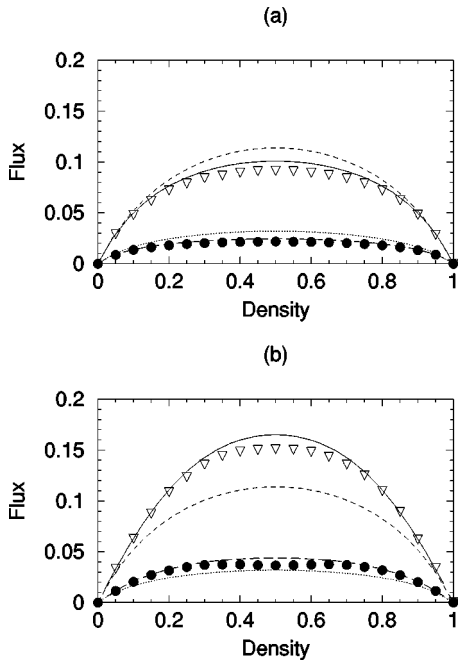

FIG. 8. Variation of the *net* flux F with the density c of the particles in the *steady state* of the two-dimensional KLS model with (a) attractive interaction $J=1.0$ and (b) repulsive interaction $J=-1.0$, both at $T=1.5T_c(E=0)$. In both (a) and (b) the discrete data points have been obtained from our computer simulations with $E=1.0$(●) and 4.0(▽), respectively. In both (a) and (b) the dotted and dashed lines represent the predictions of the 1-cluster MFT for $E=1.0$ and 4.0, respectively, while the long-dashed and solid lines represent the corresponding predictions of the 2-cluster MFT.

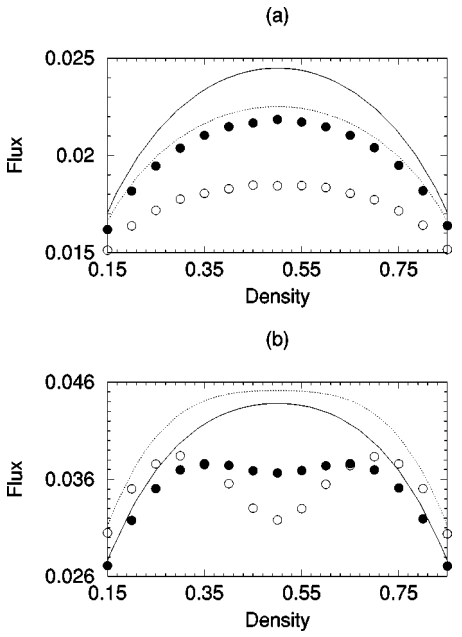

FIG. 9. Comparison of the predictions of 1-cluster and 2-cluster MFTs on the *net* flux F in the *steady-state* of the two-dimensional KLS model with (a) attractive interaction $J=1.0$ and (b) repulsive interaction $J=-1.0$, all for $E=1.0$. In both (a) and (b) the discrete data points have been obtained from our computer simulations at $T=1.25T_c(E=0)$(○) and $T=1.5T_c(E=0)$(●), respectively. In both (a) and (b) the dotted and solid lines represent the predictions of the 2-cluster MFT at $T=1.25T_c(E=0)$ and $T=1.5T_c(E=0)$, respectively.

$V_{max}=1$, where V_{max} is the largest (integer) speed allowed for each of the vehicles [6,23].

In the case of the NS model the 1-cluster MFT makes an underestimate of the flux but the 2-cluster MFT treatment is adequate to take into account the correlations introduced purely by the parallel dynamics and, therefore, it gives the exact result [15].

The KLS model can be regarded as an extension of the TASEP by incorporating nonvanishing interparticles interactions through nonzero J. Our results reported in this paper show that neither the 1-cluster MFT nor the 2-cluster MFT yield exact flux in the KLS model; although the 2-cluster results are accurate to order 10^{-3} it is the 4-cluster results that are practically indistinguishable from the corresponding computer simulation data. Although it is possible that the results of the 4-cluster MFT might be exact for the KLS model we refrain from making such a claim as we do not have any rigorous proof.

Note that in the special case,

$$E=0,$$

$$\beta J=(1/4)\ln p \quad (\text{with } 0\leqslant p<1), \tag{40}$$

we have $A=2q$, $B=-2$, and $C=2c(1-c)$ where $q=1-p$. In this case, the quadratic Eq. (18) reduces to the form $qa^2-a+c(1-c)=0$ that was derived [15] directly from the 2-cluster MF treatment of the NS model with $V_{max}=1$. Interestingly, the 2-cluster result is not exact for the KLS model, but it gives exact result for the NS model. This is a consequence of the fact that the 2-cluster MFT gives, in general exact results for the one-dimensional Ising model in equilibrium.

Since $p<1$, the relation (40) maps the NS model, with $V_{max}=1$, onto an *antiferro*magnetic Ising model, (or, equivalently, to the KLS model, with *repulsive* interparticle interactions, in the absence of external drive) so that the steady state of the former is identical to the equilibrium state of the latter. Consequently, for all densities c, we observe perfect agreement of the DH distributions in the NS model and that in the KLS model with $E=0$, $\beta J=(1/4)\ln p$ (Fig. 10).

Since the relation (40) maps the NS model (with $V_{max}=1$) onto the KLS model only for $E=0$, this mapping cannot relate the properties of the KLS model for any nonzero E with those of the NS model. Interestingly, in the NS model with $V_{max}=1$ the flux is *maximum* at $c=1/2$ for all q. In sharp contrast, the flux is *minimum* at $c=1/2$ in the KLS model with repulsive (antiferromagnetic) interactions so long as E is not much stronger than $|J|$; as E increases the depth of the well at $c=1/2$ in Fig. 2 decreases and, eventually, for sufficiently large E the flux exhibits its maximum at $c=1/2$. Moreover, the location of the maximum in the DH distribution depends crucially on the sign of the interaction J provided E is not much larger than $|J|$.

The time interval between the arrivals (or departures) of

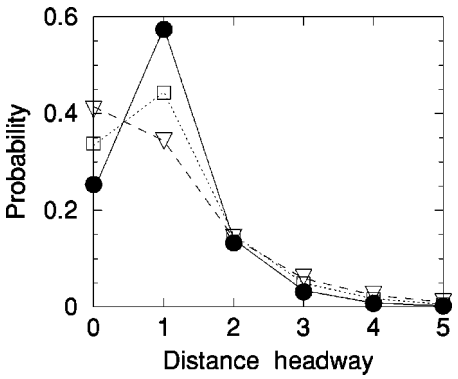

FIG. 10. The discrete data points represent the distance-headway distribution in the steady-state of the one-dimensional KLS model with repulsive interaction $J=-1.0$, for $c=1/2$ at three different values of $T=4J/(\ln p)$ corresponding, respectively, to $p=0.1$ (●), $p=0.25$ (□), and $p=0.5$ (▽), all for $E=0.0$. The lines are merely guides to the eye connecting the dots corresponding to the DH distributions in the NS model with $V_{max}=1$ and $p=0.1$ (solid line), $p=0.25$ (dotted line) and $p=0.5$ (dashed line), respectively. All the results in this figure have been obtained in the 2-cluster approximation.

the successive particles at a detector site is defined to be the corresponding time-headway (TH). The exact TH distribution for the NS model with $V_{max}=1$ has been calculated [17]. However, because of the possibility of hopping of the particles against E in the KLS model, the analytical calculation of TH distribution is extremely difficult and will not be reported here.

IX. CONCLUSION

In this paper we have reported the results of cluster-mean-field theoretic treatments of a driven-diffusive lattice gas model to calculate the flux of the particles under the influence of the driving field. Although we have considered the standard model, namely, the Katz-Lebowitz-Spohn model in this paper, our technique is sufficiently general that it can be used, in principle, to calculate the flow properties of any other driven-diffusive lattice gas.

The flux-density relations of the KLS model computed in this paper, as well as those of some closely related models [24,25], exhibit interesting double-peaked structure when the interparticle interactions are *repulsive* whereas only a single peak is observed if the interparticle interactions are attractive. We have compared our predictions, based on cluster-mean-field theories, with the corresponding Monte Carlo data; the *quantitative* agreement is excellent in $d=1$. Our investigation has helped in elucidating the roles of interparticle interactions J, temperature T and the driving field E in determining the trend of variation of the flux with the density of the particles in the driven-diffusive lattice gas models.

ACKNOWLEDGMENTS

One of us (D.C.) would like to thank the Department of Computational Science of the National University of Singapore for hospitality during a short visit where this paper was completed. We also thank A. Schadschneider and A. Szolnoki for useful correspondence.

APPENDIX A

Concrete examples of exact master equations for n-cluster probabilities in the one-dimensional KLS model,

$$\frac{dP_2(0,0)}{dt} = -\min[1,e^{-\beta(E+4J)}]P_4(0,0,1,1) + \min[1,e^{\beta(E+4J)}]P_4(0,1,0,1) + \min[1,e^{\beta(-E+4J)}]P_4(1,0,1,0) - \min[1,e^{\beta(E-4J)}]P_4(1,1,0,0), \quad \text{(A1)}$$

$$\frac{dP_3(0,0,0)}{dt} = -\min[1,e^{-\beta E}]P_5(0,0,0,1,0) - \min[1,e^{-\beta(E+4J)}]P_5(0,0,0,1,1) + \min[1,e^{-\beta E}]P_5(0,0,1,0,0) + \min[1,e^{\beta E}]P_5(0,0,1,0,0) + \min[1,e^{\beta(E+4J)}]P_5(0,0,1,0,1) - \min[1,e^{\beta E}]P_5(0,1,0,0,0) + \min[1,e^{\beta(-E+4J)}]P_5(1,0,1,0,0) - \min[1,e^{\beta(E-4J)}]P_5(1,1,0,0,0). \quad \text{(A2)}$$

APPENDIX B

Exact master equations for the 4-cluster probabilities in the one-dimensional KLS model,

$$\left[\frac{dP_4(c_{i-1},c_i,c_{i+1},c_{i+2})}{dt}\right] = \sum_{\tau_{i-2},\tau_{i+3}} [P_6(\tau_{i-2},c_{i-1},c_{i+1},c_i,c_{i+2},\tau_{i+3})w(c_{i-1},c_{i+1},c_i,c_{i+2}) - P_6(\tau_{i-2},c_{i-1},c_i,c_{i+1},c_{i+2},\tau_{i+3})w(c_{i-1},c_i,c_{i+1},c_{i+2})] + \sum_{\tau_{i-2},\tau_{i+3}} [P_6(\tau_{i-2},c_{i-1},c_i,c_{i+2},c_{i+1},\tau_{i+3})w(c_{i-1},c_i,c_{i+2},c_{i+1})$$

$$
\begin{aligned}
&- P_6(\tau_{i-2}, c_{i-1}, c_i, c_{i+1}, c_{i+2}, \tau_{i+3}) w(c_{i-1}, c_i, c_{i+1}, c_{i+2})] \\
&+ \sum_{\tau_{i-2}, \tau_{i+3}} [P_6(\tau_{i-2}, c_i, c_{i-1}, c_{i+1}, c_{i+2}, \tau_{i+3}) w(c_i, c_{i-1}, c_{i+1}, c_{i+2}) \\
&- P_6(\tau_{i-2}, c_{i-1}, c_i, c_{i+1}, c_{i+2}, \tau_{i+3}) w(c_{i-1}, c_i, c_{i+1}, c_{i+2})] \\
&+ \sum_{\tau_{i+3}, \tau_{i+4}} [P_6(c_{i-1}, c_i, c_{i+1}, \tau_{i+3}, c_{i+2}, \tau_{i+4}) w(c_{i+1}, \tau_{i+3}, c_{i+2}, \tau_{i+4}) \\
&- P_6(c_{i-1}, c_i, c_{i+1}, c_{i+2}, \tau_{i+3}, \tau_{i+4}) w(c_{i+1}, c_{i+2}, \tau_{i+3}, \tau_{i+4})] \\
&+ \sum_{\tau_{i-2}, \tau_{i-3}} [P_6(\tau_{i-3}, c_{i-1}, \tau_{i-2}, c_i, c_{i+1}, c_{i+2}) w(\tau_{i-3}, c_{i-1}, \tau_{i-2}, c_i) \\
&- P_6(\tau_{i-3}, \tau_{i-2}, c_{i-1}, c_i, c_{i+1}, c_{i+2}) w(\tau_{i-3}, \tau_{i-2}, c_{i-1}, c_i)]. \qquad \text{(B1)}
\end{aligned}
$$

[1] B. Schmittmann and R. K. P. Zia, in *Phase Transitions and Critical Phenomena*, edited by C. Domb and J. L. Lebowitz (Academic Press, New York, 1995), Vol. 17; Phys. Rep. **301**, 45 (1998); R. K. P. Zia and L. B. Shaw, B. Schmittmann, and R. J. Astalos, e-print cond-mat/9906376.

[2] G. Schütz, in *Phase Transitions and Critical Phenomena*, edited by C. Domb and J. L. Lebowitz (Academic Press, New York, 2000), Vol. 19.

[3] *Nonequilibrium Statistical Mechanics in One Dimension*, edited by V. Privman (Cambridge University Press, Cambridge, 1997).

[4] J. Marro and R. Dickman, *Nonequilibrium Phase Transitions in Lattice Models* (Cambridge University Press, Cambridge, 1999).

[5] S. Katz, J. L. Lebowitz, and H. Spohn, Phys. Rev. B **28**, 1655 (1983); J. Stat. Phys. **34**, 497 (1984).

[6] D. Chowdhury, L. Santen, and A. Schadschneider, Phys. Rep. **329**, 199 (2000).

[7] D. Helbing, e-print cond-mat/0012229.

[8] *Traffic and Granular Flow*, edited by D. E. Wolf, M. Schreckenberg, and A. Bachem (World Scientific, Singapore, 1996); *Traffic and Granular Flow '97*, edited by M. Schreckenberg and D. E. Wolf (Springer, Singapore, 1998); *Traffic and Granular Flow '99*, edited by D. Helbing, H. J. Herrmann, M. Schreckenberg, and D. E. Wolf (Springer, Berlin, 2000).

[9] A. D. May, *Traffic Flow Fundamentals* (Prentice-Hall, Englewood Cliffs, NJ, 1990).

[10] R. Dickman, Phys. Rev. A **34**, 4246 (1986); **38**, 2588 (1988); **41**, 2192 (1990).

[11] N. C. Pesheva, Y. Shnidman, and R. K. P. Zia, J. Stat. Phys. **70**, 737 (1993).

[12] G. Szabó, A. Szolnoki, and L. Bodócs, Phys. Rev. A **44**, 6375 (1991).

[13] A. Szolnoki and G. Szabó, Phys. Rev. E **48**, 611 (1993).

[14] G. Szabó and A. Szolnoki, Phys. Rev. E **49**, 299 (1994); **53**, 196 (1996).

[15] M. Schreckenberg, A. Schadschneider, K. Nagel, and N. Ito, Phys. Rev. E **51**, 2939 (1995); A. Schadschneider, and M. Schreckenberg, J. Phys. A **26**, L679 (1993); A. Schadschneider, Eur. Phys. J. B **10**, 573 (1999).

[16] D. Chowdhury, A. Majumdar, K. Ghosh, S. Sinha, and R. B. Stinchcombe, Physica A **246**, 471 (1997).

[17] K. Ghosh, A. Majumdar, and D. Chowdhury, Phys. Rev. E **58**, 4012 (1998); D. Chowdhury, A. Pasupathy, and S. Sinha, Eur. Phys. J. B **5**, 781 (1998).

[18] J. S. Wang, J. Stat. Phys. **82**, 1409 (1996).

[19] H. Spohn, *Large Scale Dynamics of Interacting Particles* (Springer, New York, 1991).

[20] B. Derrida and M. R. Evans, in *Non-Equilibrium Statistical Mechanics in One Dimension*, edited by V. Privman (Cambridge University Press, Cambridge, 1997); B. Derrida, Phys. Rep. **301**, 65 (1998).

[21] A. Szolnoki (private communication); we are indebted to Dr. Szolnoki for drawing our attention to this relation.

[22] K. Nagel and M. Schreckenberg, J. Phys. I **2**, 2221 (1992).

[23] L. Gray and D. Griffeath, J. Stat. Phys. **105**, 413 (2001).

[24] G. Szabó, A. Szolnoki, Z. Juhász, and G. Ódor, Physica A **191**, 445 (1992).

[25] J. S. Hager, J. Krug, V. Popkov, and G. M. Schütz, Phys. Rev. E **63**, 056110 (2001); J. S. Hager, *ibid.* **63**, 067103 (2001).